

1 **Single-cell transcriptome profiling reveals dermal and epithelial
2 cell fate decisions during embryonic hair follicle development**

3 Wei Ge¹, Shao-Jing Tan², Shan-He Wang¹, Lan Li², Xiao-Feng Sun², Wei Shen^{2,¶}, Xin
4 Wang^{1,¶}

5

6 *1. Key Laboratory of Animal Genetics, Breeding and Reproduction of Shaanxi Province,
7 College of Animal Science and Technology, Northwest A&F University, Yangling, Shaanxi
8 712100, China;*

9 *2. College of Life Sciences, Qingdao Agricultural University, Qingdao 266109, China.*

10

11

12

13 ¶ Correspondence and reprint requests to:

14 Prof. Wei Shen; E-mail: wshen@qau.edu.cn; shenwei427@163.com

15 Prof. Xin Wang; E-mail: wxwza@126.com

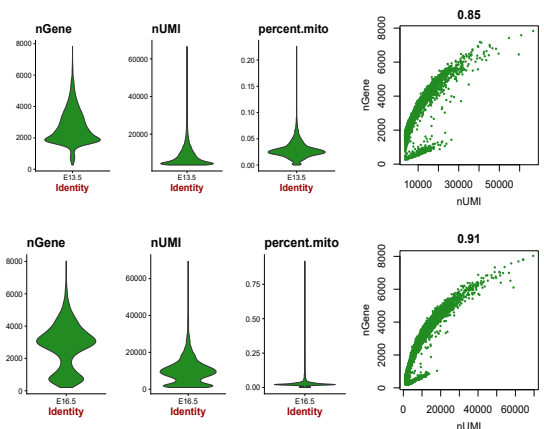
16

Supplementary Figure 1

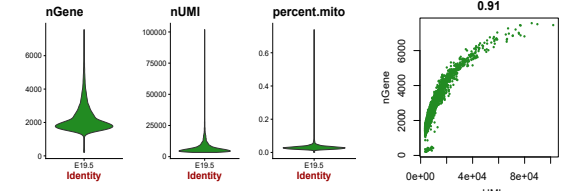
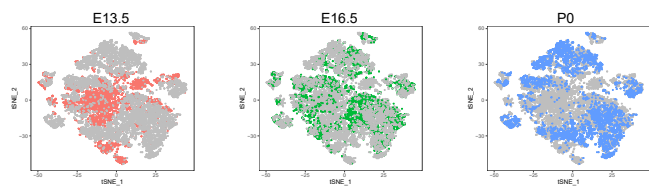
A

Sample info.	E13.5	E16.5	P0
Estimated Number of Cells	7,000	7,000	7,000
Valid Barcodes	97.2%	97.3%	97.6%
Mean Reads per Cell	75,538	77,370	75,560
Median Genes per Cell	2,434	2,978	1,989
Total Genes Detected	19,997	19,767	19,145
Reads Mapped to Genome	90.5%	91.5%	94.0%
Reads Mapped Confidently to Transcriptome	62.8%	65.2%	71.7%

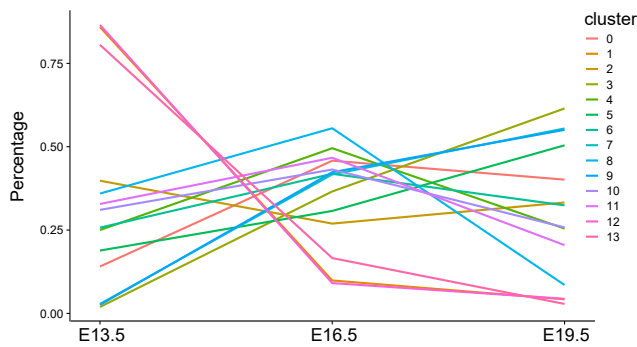
B



C



D

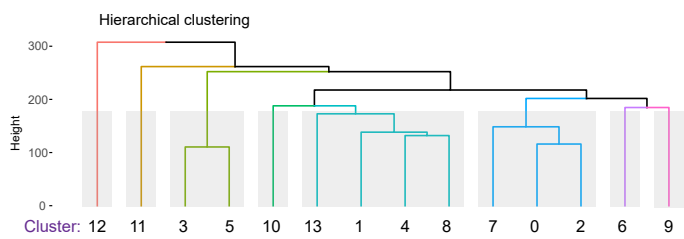


17 **Figure S1: Quality control of single-cell data.** (A) Single cell datasets quality metrics
18 summary identified by CellRanger. (B) Violin plot displaying the number of genes (nGene),
19 UMI (nUMI), and percentage of mitochondrial genes (percent.mito) detected in all single
20 cells from three different datasets. The gene to UMI relationship for each dataset was also
21 visualized. Generally, the more UMI captured, the more genes detected. (C) tSNE plot
22 labeled by developmental timepoint. (D) Line-plot demonstrating the percentage of cells
23 from different time-points in each cluster.

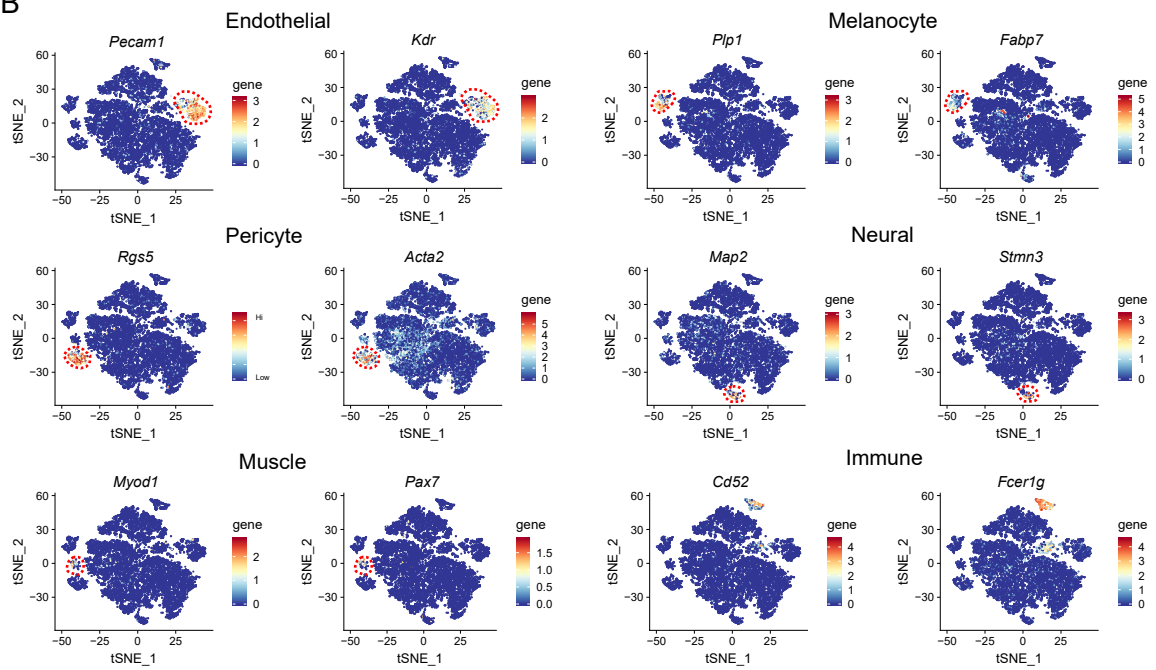
24

Supplementary Figure 2

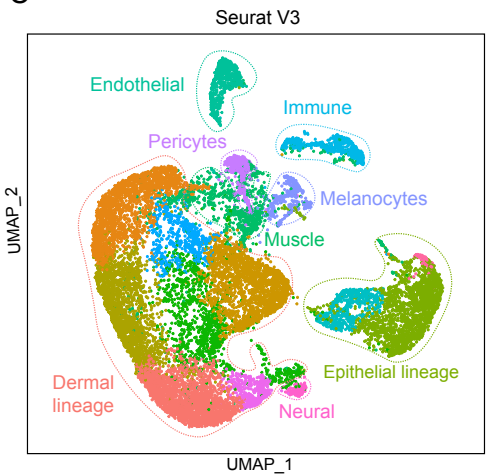
A



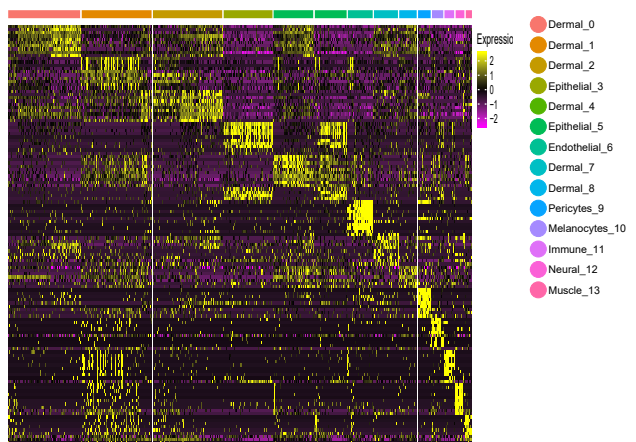
B



C

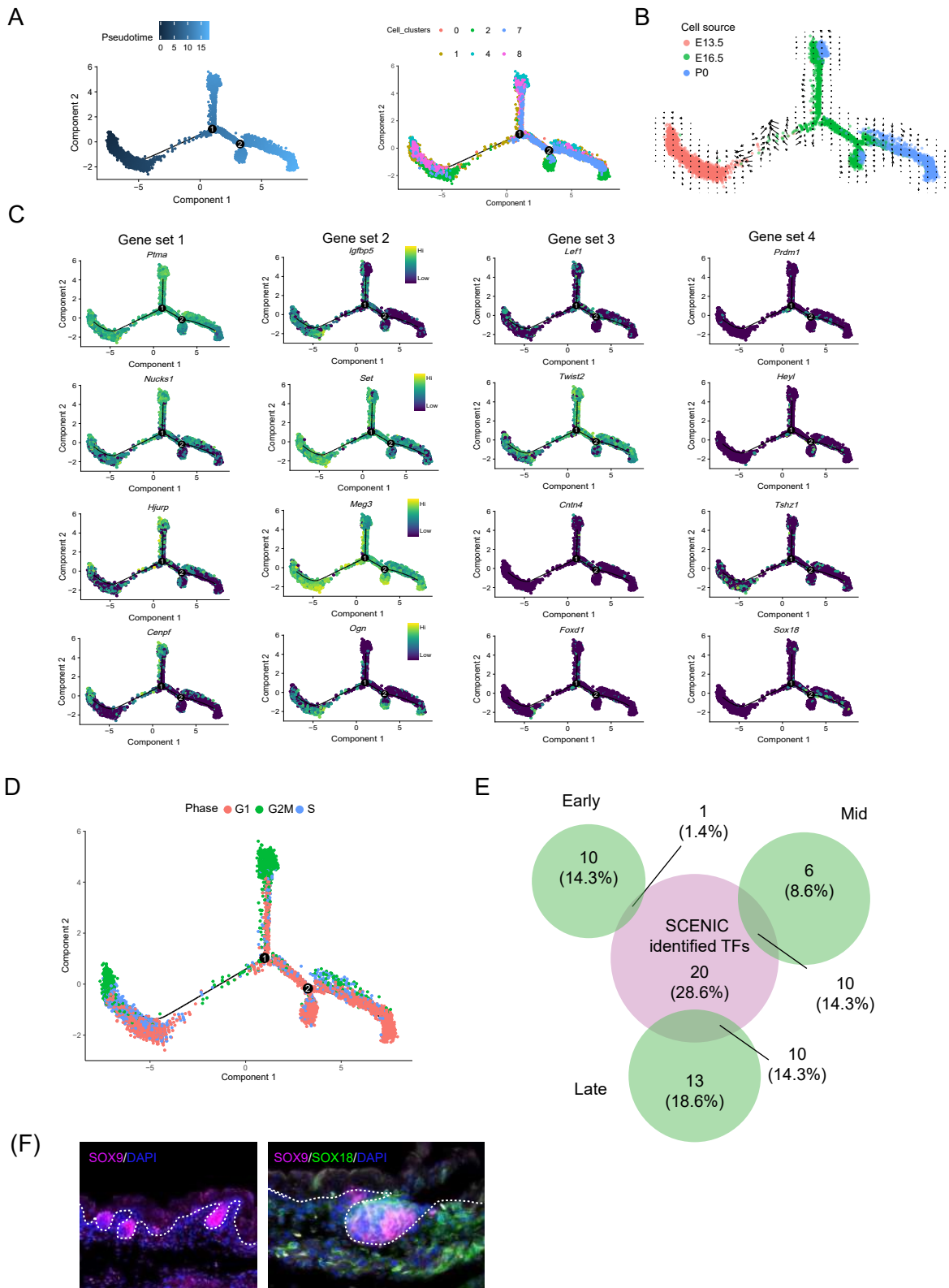


D



25 **Figure S2: Characterization of major cell populations in the embryonic skin.** (A)
26 Hierarchical clustering of different cell clusters identified by tSNE. the cluster number was
27 in accordance with Figure 1B. (B) Visualization of canonical marker gene expression in the
28 tSNE plot of all single cells. Endothelial markers: *Pecam1*, *Kdr*; Melanocyte markers: *Plp1*,
29 *Fabp7*; Pericyte markers: *Rgs5*, *Acta2*; Neural markers: *Map2*, *Stmn3*; Muscle markers:
30 *Myod1*, *Pax7*, Immune markers: *Cd52*, *Fcer1g*. (C) Dimension reduction analysis using
31 Seurat V3 pipeline. (D) Heatmap displaying top 10 signature gene expression in each
32 cluster.
33

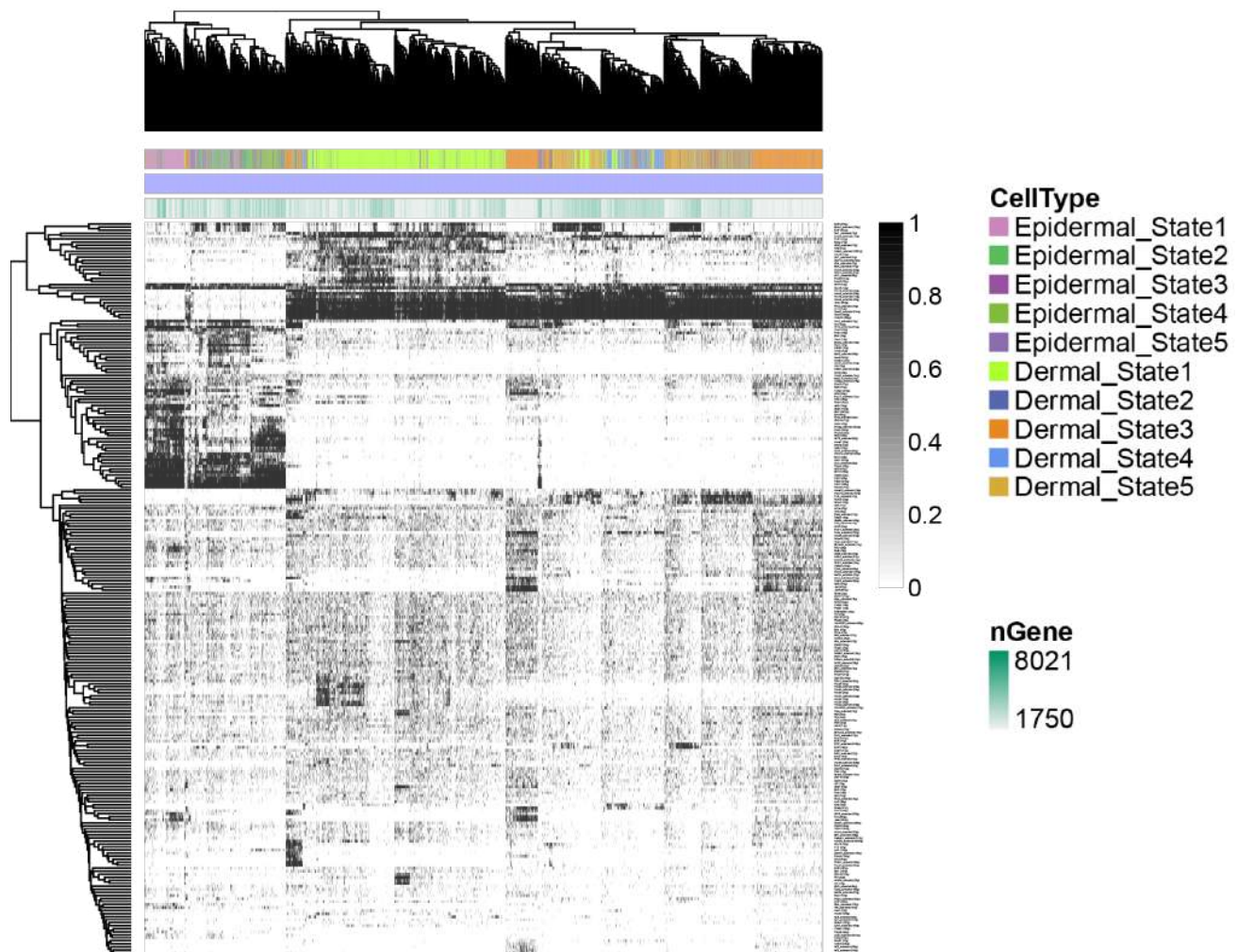
Supplementary Figure 3



34 **Figure S3: Visualization of key DC markers expression.** (A) Pseudotime ordering
35 analysis of all dermal populations, cells were labeled with pseudotime (left) and their
36 corresponding cluster information (right), respectively. (B) RNA velocity vectors
37 incorporated in the Monocle pseudotime trajectory. (C) Visulizing representative gene
38 expression along pseudotime. (D) Visualizing cell cycle progression in the Monocle
39 pseudotime trajectory. (E) Venn diagram showing overlapped transcriptional factors
40 between this paper and Mok et al. Early, middle, and late represent different stages during
41 hair follicle DC specification. (F) Immunofluorescence analysis of SOX9 and SOX18
42 expression in E16.5 skin tissues.

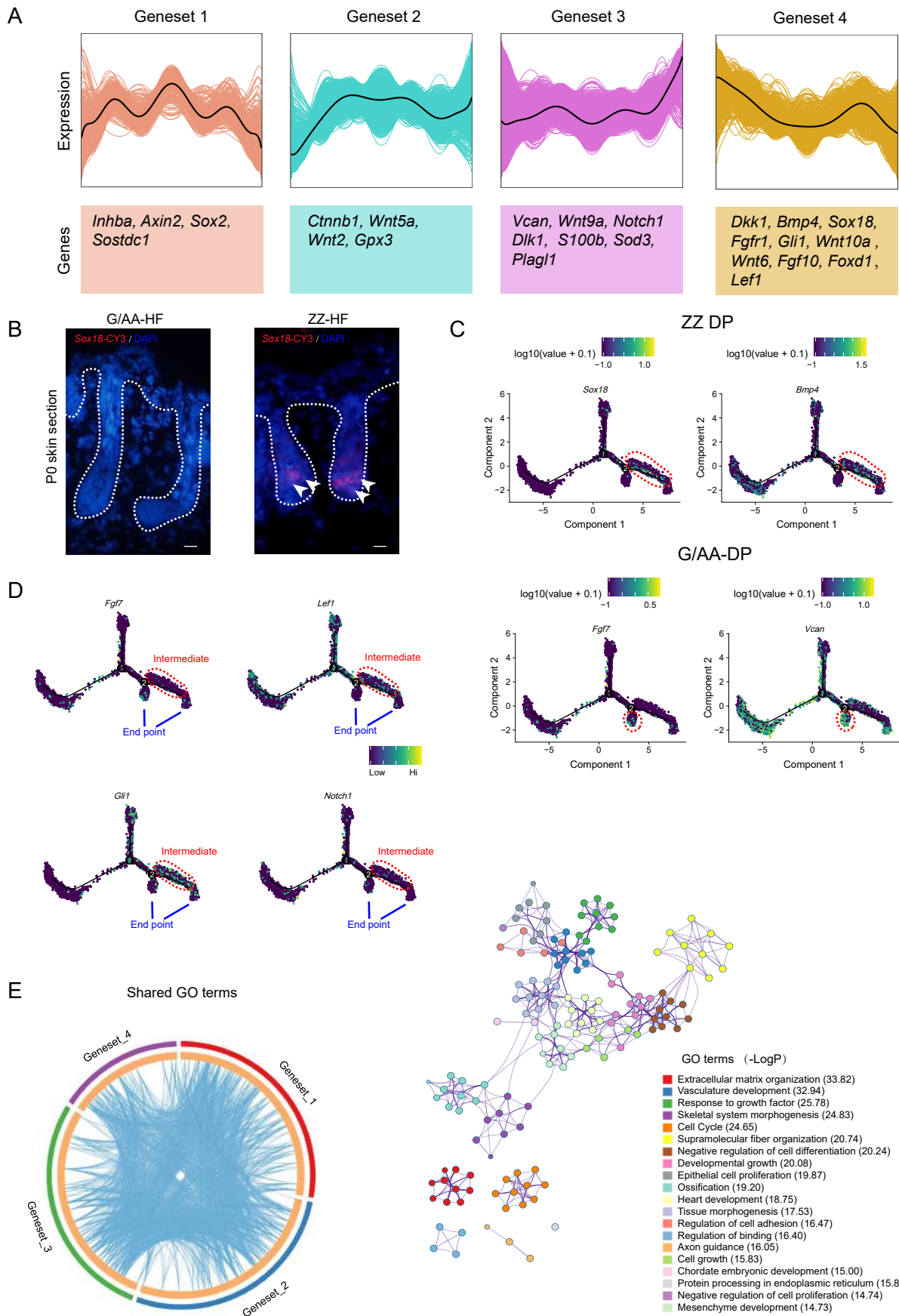
43

Supplementary Figure 4



44 **Figure S4:** SCENIC binary regulon activity heatmap depicting all dermal and epidermal
45 cell states-specific enriched regulons.

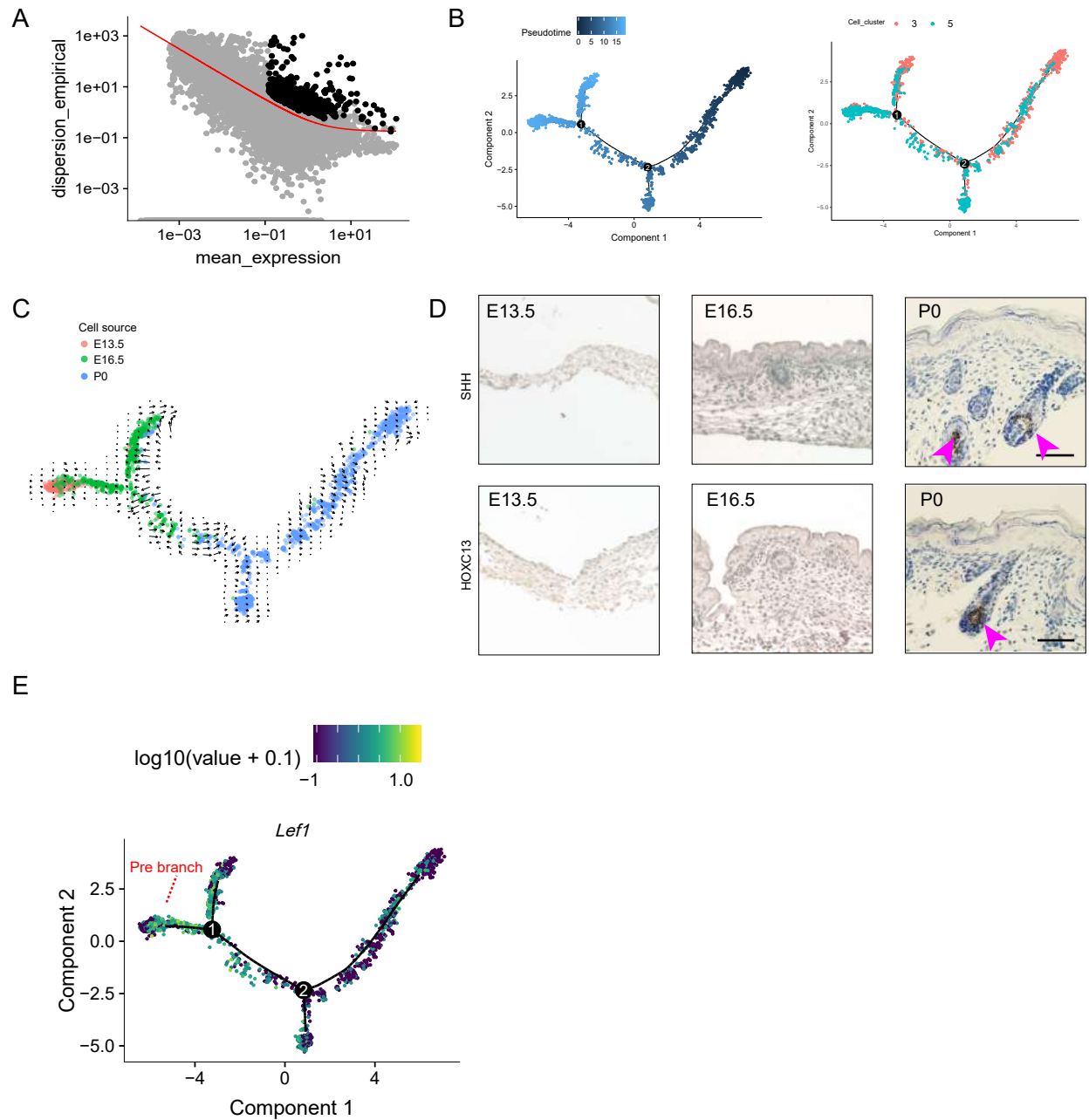
Supplementary Figure 5



46 **Figure S5: Investigating gene expression profile during AA/ZZ DP and G-DP fate**
47 **commitment** (A) Gene expression profile and representative genes during AA/ZZ DP and
48 G-DP fate commitment. (B) mRNA ISH of *Sox18* in P0 skin tissue. (C) Representative
49 AA/ZZ DP and G-DP marker expression projected into pseudotime trajectory. (D)
50 Comparison of *Fgf7*, *Lefl*, *Gli1*, and *Notch1* expression in the pseudotime trajectory. The
51 red dotted box depicts an intermediate stage, while the blue line indicates the endpoint. (E)
52 Circos plot indicating the shared GO terms and GO interaction network constructed from
53 different gene set enriched GO terms. Different colors in the network depict different GO
54 terms.

55

Supplementary Figure 6

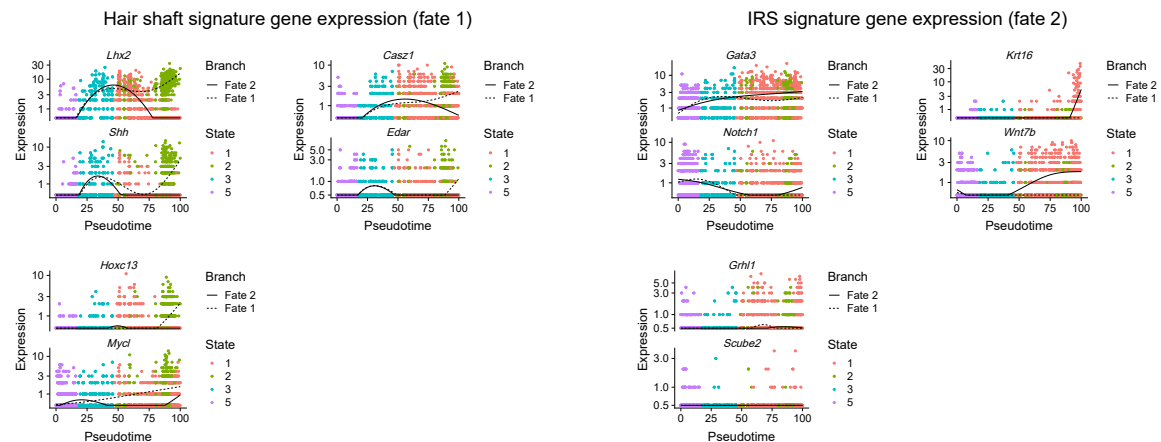


56 **Figure S6: Interpreting IFE and matrix molecular signature** (A) Scatter plot of mean
57 expression against the empirical dispersion displaying the variable genes (black dots) used
58 for Monocle pseudotime ordering. (B) Pseudotime ordering analysis of all epithelium
59 populations, cells were labeled with pseudotime (left) and their corresponding cluster
60 information (right), respectively. (C) RNA velocity vectors incorporated in the Monocle
61 pseudotime trajectory. Cells were color-coded with their corresponding developmental
62 timepoint. (D) Immunohistochemistry validation of SHH and HOXC13 expression in E13.5,
63 E16.5 and P0 skin tissues. Scale bar, 50 μ m. (F) Visualization of *Lef1* expression projected
64 into pseudotime trajectory.

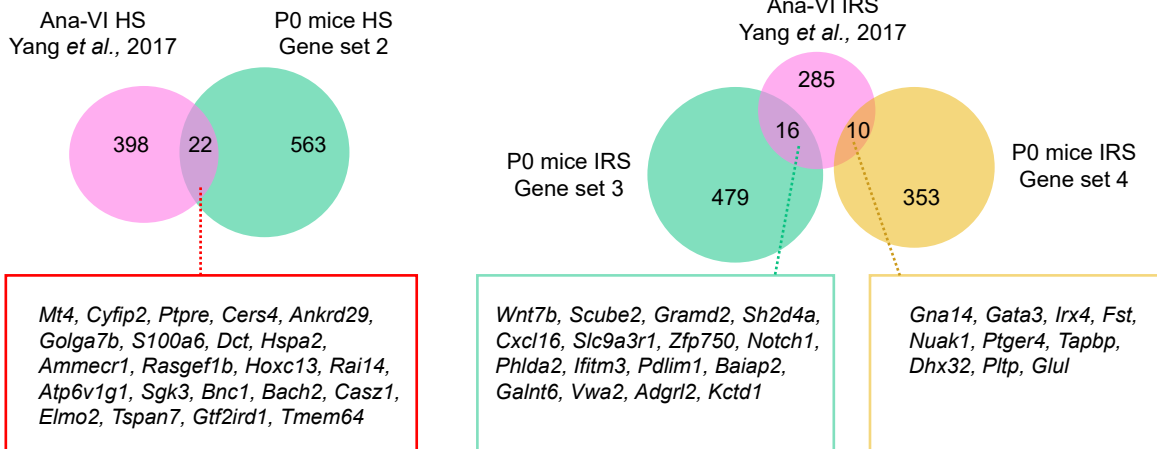
65

Supplementary Figure 7

A



B



66 **Figure S7: Dissecting hair shaft and IRS fate decisions.** (A) Hair shaft and IRS signature
67 gene expression along pseudotime. Cells were labeled with cell states with a solid line
68 indicating fate 2 and a dotted line indicating fate 1. (B) Comparison of HS and IRS
69 signature genes between Anagen VI from Yang et al., and our single cell analysis here. The
70 overlapped genes were listed in the rectangular box.
71

72 **Supplementary Tables:**

73 **Table S1.** List of DEGs for tSNE identified 13 clusters. Corresponding to Figure 1B.

74 **Table S2.** List of branch-specific DEGs expression along pseudotime. Corresponding to
75 Figure 2C.

76 **Table S3.** List of SCENIC enriched TFs and it's corresponding targets.

77 **Table S4.** Signature genes comparison P0 G-DP, AA/ZZ DP (this study) and AA/ZZ DP, ZZ
78 DP, GAA DP, G-DP (Rezza et al.). Corresponding to Figure 3D.

79 **Table S5.** Signature genes comparison P0 hair shaft/IRS (this study) and anagen VI HS/IRS
80 (Yang et al. 2017).

81